Geomorphology 214 (2014) 139–147

Contents lists available at ScienceDirect

Geomorphology

journal homepage: www.elsevier.com/locate/geomorph

Basal roughness of the Institute and Möller Ice Streams, West Antarctica: Process determination and landscape interpretation

D.M. Rippin [a,*], R.G. Bingham [b], T.A. Jordan [c], A.P. Wright [d], N. Ross [e], H.F.J. Corr [c], F. Ferraccioli [c], A.M. Le Brocq [d], K.C. Rose [f], M.J. Siegert [f]

[a] Environment Department, University of York, UK
[b] School of Geosciences, University of Edinburgh, UK
[c] British Antarctic Survey, Madingley Road, Cambridge, UK
[d] Geography, College of Life and Environmental Sciences, University of Exeter, UK
[e] School of Geography, Politics and Sociology, Newcastle University, UK
[f] School of Geographical Sciences, University of Bristol, UK

ARTICLE INFO

Article history:
Received 18 July 2013
Received in revised form 27 January 2014
Accepted 28 January 2014
Available online 12 February 2014

Keywords:
Antarctica
Roughness
Radio-echo sounding
Ice dynamics
Möller Ice Stream
Institute Ice Stream

ABSTRACT

We present a detailed analysis of bed roughness beneath Institute and Möller Ice Streams, west Antarctica, using radio-echo sounding data (RES) acquired in the austral summer of 2010/11. We assess roughness using a two-parameter approach and also assess the directionality of roughness relative to present-day ice flow. Our work highlights the wealth of additional information that resides in analyses of bed roughness. Employing these multiple approaches we show that spatially variable roughness patterns are partly a consequence of the ability of flowing ice not only to smooth the bed but also to redistribute and remove sediments, and to do this along-flow. Accordingly, we identify some fast-flow tributaries underlain by topography that has been streamlined and other tributaries that are underlain by sediments. We also identify locations that are currently protected from erosion, but where more ancient erosion may once have occurred. We conclude that detailed roughness analysis is a useful tool for landscape interpretation; and we suggest that the roughness of an ice-sheet's bed should be viewed not only as the consequence of ancient marine sedimentation, but also as a product of more contemporary erosion and redistribution of sediments, as well as bedrock-smoothing that is ongoing because of continuing dynamic activity. In this way, basal roughness has the potential to evolve continually with ice sheet form and flow, and should not be viewed simply as a snapshot of either present-day or palaeo-basal conditions.

1. Introduction

In terms of its width and discharge, the Institute Ice Stream (IIS) is one of the biggest of Antarctica's glaciers (Scambos et al., 2004). Through it, and also the adjacent Möller Ice Stream (MIS), a very significant proportion of the West Antarctic Ice Sheet (WAIS) drains toward the Ronne Ice Shelf (Fig. 1). The substantial role that these two ice streams have in draining the WAIS means that changes in their behaviour have the potential to impact significantly upon the mass balance of the WAIS as a whole (Scambos et al., 2004; Bingham and Siegert, 2007). However, despite their importance, our knowledge of the history of ice flow in this region is less developed than in other parts of Antarctica. Until recently, studies of the area were based on reconnaissance airborne radio-echo sounding (RES) data collected between 1977 and 1979 in which along-flightline bed-sampling was sparse (~2 km), so that only a very broad idea of subglacial topography from the area was resolved (Thiel, 1961; Drewry and Meldrum, 1978; Drewry et al., 1980; Jankowski and Drewry, 1981; Drewry, 1983). Analysing these data for regional-scale basal roughness, Bingham and Siegert (2007) noted that subglacial topography across the region graduated from rougher toward the divides to smoother downstream. In particular, the remarkable smoothness of the bed toward the grounding zones of IIS and MIS was identified as analogous to the smooth bed beneath the Siple Coast ice streams draining to the Ross Ice Shelf. There, smooth beds correspond to the inferred presence of extensive marine sediments that, in turn, can facilitate rapid variations in ice-flow

* Corresponding author. Tel.: +44 1904 324 703.
E-mail addresses: david.rippin@york.ac.uk (D.M. Rippin), r.bingham@ed.ac.uk (R.G. Bingham), tomj@bas.ac.uk (T.A. Jordan), wright.andy.p@googlemail.com (A.P. Wright), Neil.Ross@newcastle.ac.uk (N. Ross), hfjc@bas.ac.uk (H.F.J. Corr), ffe@bas.ac.uk (F. Ferraccioli), A.LeBrocq@exeter.ac.uk (A.M. Le Brocq), K.C.Rose@bristol.ac.uk (K.C. Rose), M.J.Siegert@bristol.ac.uk (M.J. Siegert).

http://dx.doi.org/10.1016/j.geomorph.2014.01.021
0169-555X/

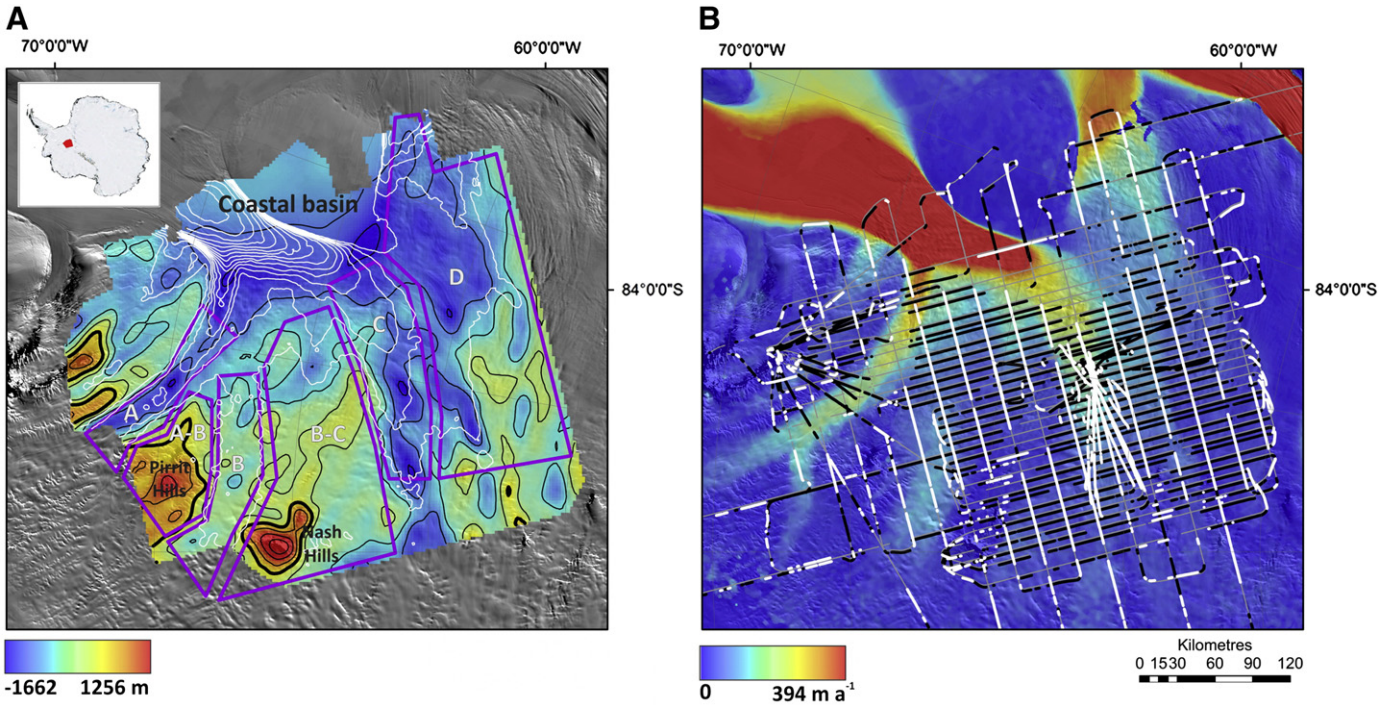

Fig. 1. Detailed maps of Institute and Möller Ice Streams in West Antarctica. (A) Background is a MODIS image with bed topography overlain in colour (and with thin black contour (400-m) lines) derived from our data (cf., Ross et al., 2012). The thick black contour represents current sea level. SAR-derived ice velocities (after Rignot et al., 2011) are visible as white contours (25 ma^{-1}) and clearly delineate the margins of IIS and MIS. Purple boxes outline the roughness subregions discussed later in the text. White letters within these boxes (areas A, B, C, and D) define regions incorporating tributaries of MIS and IIS; areas A–B and B–C are intertributary areas. The inset is a location map showing the study region in Antarctica. (B) Ice velocity (after Rignot et al., 2011) semitransparent over the MODIS image shown in (A). Overlying these are flightlines — the full data set is shown in grey, and lines are shaded white where they are parallel to flow and black where they are orthogonal to flow.

speed, ice-stream configuration and mass balance (Fahnestock et al., 2000; Kamb, 2001; Hulbe and Fahnestock, 2007; Catania et al., 2012).

In this paper, we reconsider the basal conditions of IIS and MIS by analysing the roughness of the basal interface recovered from a new high-resolution RES data set acquired over the region in the austral summer of 2010/11. We are motivated by the increased recognition of basal roughness as an indicator of subglacial conditions and as a potential control on ice-sheet dynamics or indicator of past ice-sheet dynamism. A generalized scheme for using basal roughness as an indicator of regional subglacial conditions across Antarctica was presented by Bingham and Siegert (2009). This demonstrates, for example, that smooth beds are often associated with the presence of subglacial sediments that can smother bedrock obstacles that would otherwise increase basal friction. Subglacial sediments also have the ability to deform which can further enhance ice streaming (e.g. Tulaczyk et al., 1998). In terms of controls on ice dynamics, a rougher bed provides greater resistance to flow over it, whereas a smooth bed facilitates faster flow (e.g., Siegert et al., 2004, 2005; Peters et al., 2005; Rippin et al., 2006). In some cases, smooth beds now lying outwith current areas of fast flow may be taken as signals of the past presence of fast flow over those areas (e.g. Bingham et al., 2007).

While ways in which the roughness of surfaces can be measured are numerous, a method that has proven particularly effective at characterising the nature of glacially modified surfaces employs a form of spectral analysis centred around Fast Fourier Transforms (FFTs) (e.g. Taylor et al., 2004; Bingham and Siegert, 2007; Rippin et al., 2011). We employ this method here to analyse the roughness of the bed beneath IIS and MIS, but our analysis conveys two critical advantages over previous work (c.f., Bingham and Siegert, 2007). Firstly, the new data from IIS and MIS allow us to determine basal roughness with much higher resolution, thereby providing much greater insight into the overall basal conditions. Secondly, we take advantage of recent developments in the methods of basal roughness analysis that have occurred since the publication of the earlier study (Li et al., 2010; Wright et al., 2012). We use these developments to analyse two components of the bed roughness signal and also to recover directionality of roughness in order to aid discrimination between predominantly erosional and predominantly depositional surfaces at the bed of the ice in different locations across IIS and MIS.

2. Data and methods

2.1. Survey

In the austral summer 2010/11, >25 000 km of airborne RES data were collected over IIS and MIS (Fig. 1) using the ice-sounding system PASIN (Polarimetric Airborne Survey Instrument). The PASIN system is a coherent radar with a centre frequency of 150 MHz, and surveys were conducted using a stepped survey design to minimise data collection at terrain clearances above 500 m. Ross et al. (2012) outlined the wider objectives of the aerogeophysical survey, while further details concerning the operation of the PASIN RES system are given in Vaughan et al. (2006), Corr et al. (2007), Hélière et al. (2007) and Rippin et al. (2011). Differential GPS was used for positioning with a horizontal accuracy of ~5 cm. Returns from bed reflections were picked and processed using a semiautomatic procedure within the software package PROMAX. Doppler processing was also used to migrate the radar data in the along-track direction. A more complete explanation of the Doppler processing involved is outlined in Hélière et al. (2007). Ice thickness was determined at along-track intervals of ~10 m, using a velocity of 0.168 m ns^{-1}. Finally, bed elevations were determined by subtracting ice thickness measurements from ice surface elevations, determined from measurements of terrain clearance derived from radar/laser altimeter measurements (Ross et al., 2014). Using the above approach, the topography of the bed in this region of West Antarctica has been resolved with much enhanced detail, revealing the presence of a significant coastal

subglacial basin and a well-defined network of subglacial mountains and valleys that are likely to have exploited preexisting geological structures (Ross et al., 2012; Jordan et al., 2013; Ross et al., 2014). Analysing the roughness of this subglacial landscape forms the central methodological objective of this paper.

2.2. Two-parameter FFT roughness

Roughness can be defined as the extent to which terrain varies vertically over a given horizontal distance (cf., Siegert et al., 2004, 2005; Taylor et al., 2004; Rippin et al., 2006, 2011; Bingham and Siegert, 2007, 2009; Bingham et al., 2007). Examples of rougher and smoother terrain, identifiable in RES data are shown in Fig. 2.

The FFTs can be used to quantify surface roughness over a range of wavelengths. Originally applied to interpreting submetre-scale deglaciated landforms in the proglacial foreground of an alpine glacier (Hubbard et al., 2000), the FFT technique was upscaled to the analysis of sub-ice-sheet landscapes by Taylor et al. (2004). It has subsequently been used to derive bed roughness beneath a number of regions of Antarctica (e.g. Siegert et al., 2004, 2005; Bingham et al., 2007; Rippin et al., 2011) and Greenland (Rippin, 2013). Over time, however, the technique has been refined. Of particular significance, Li et al. (2010) noted that the adoption of a second roughness parameter from FFT helps to narrow down interpretations of basal conditions from basal roughness analysis. Their 'two parameter' FFT index enables not just the traditional measure of roughness (which is effectively a relative measure of bed obstacle amplitude or vertical roughness), but also provides an indication of the frequency of roughness obstacles. However, that this term is in fact rather misleading is important to note, as the value is high when long wavelength (low frequency) obstacles dominate, and it is low when short wavelength (high frequency) obstacles dominate (Wright et al., 2012). To describe this variable as indicating the wavelength of roughness obstacles is therefore more accurate.

Li et al. (2010) outlined how, together, these two parameters enable the characterisation of subglacial process domains operating at the glacier bed, discrimination between whether the bed is one of bedrock or marine sediments, and clarification as to whether it is predominantly an erosional or a depositional environment. Such a two-parameter index was adopted by Wright et al. (2012) in their analysis of the basal roughness beneath the Aurora Subglacial basin, East Antarctica. Here, we use the same method and, for clarity, list the major steps involved below.

- In order for FFT to be carried out, the along-track data need to be continuous (i.e. with no gaps). To find missing points in RES track data is

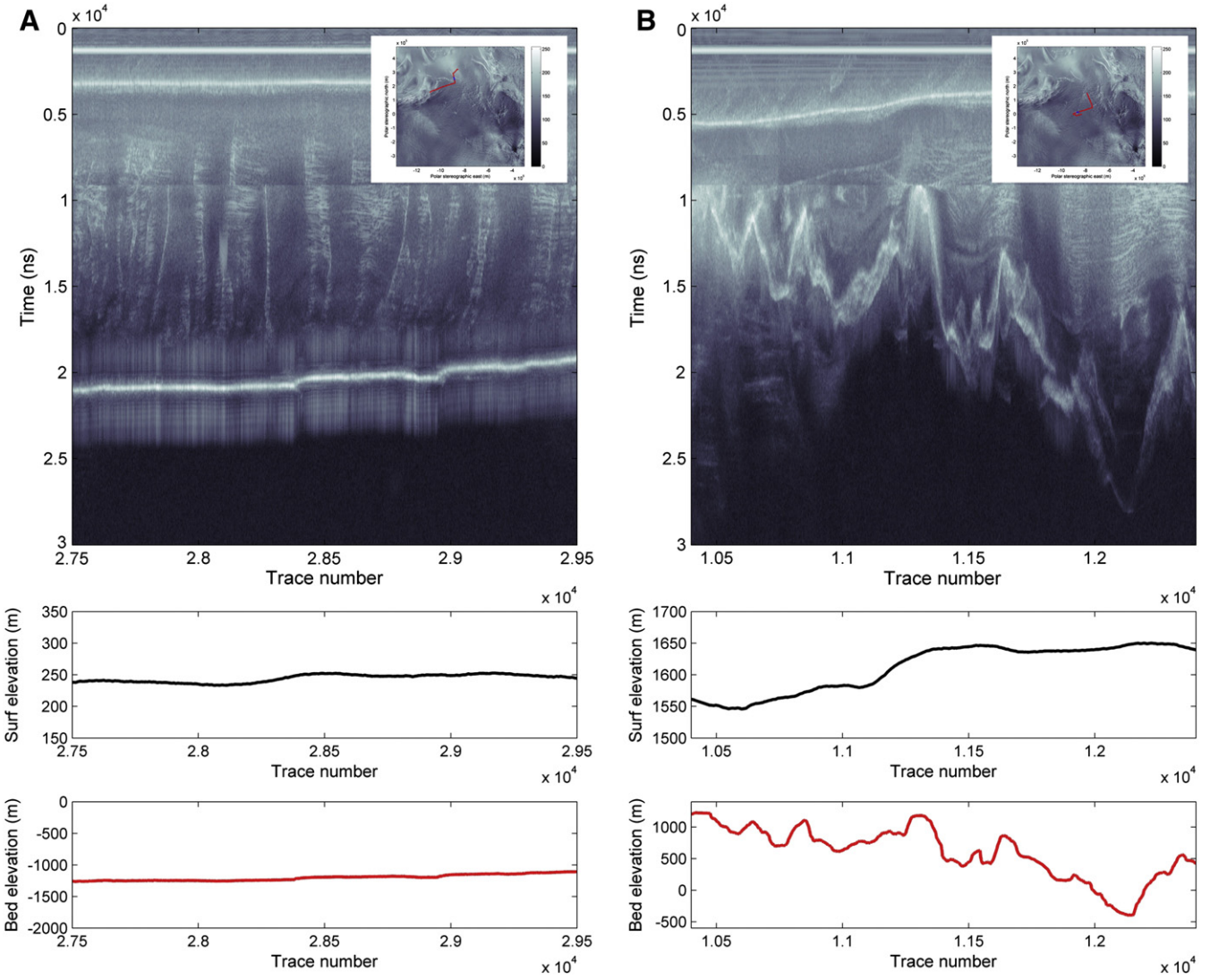

Fig. 2. Example 20-km-long SAR-processed radargrams of (A) smooth and (B) rough terrain from beneath our study area. The top panel shows the radargram, and below this are the surface and bed profiles, respectively. Inset shows sections (blue) of each flightline (red) from which these sample radargrams are taken.

not unusual, and so where any gaps are small, we use a linear interpolation to fill them. We define that a 'small' gap contains fewer than 10 consecutive missing points that, at a mean step-size of ~10 m (cf., Ross et al., 2014), means that if a gap is <100 m in length, then we interpolate across it. Where there was a gap of 10 or more points, the line was identified as being 'broken', and we determined that no FFT analysis should take place across it. Instead, analysis recommenced farther down-profile beyond the identified gap.

- Another requirement for successful application of this FFT procedure is that the data are equally spaced. As a consequence, continuous sections of line were resampled at a regular 10-m step size. This is important so that subsequent smoothing of the data can be carried out over a consistent distance.
- The mean of the bed topography was subtracted in order to remove large-scale variations in topography. This was carried out by subtracting the mean elevation over a window the same size as the FFT window (see below).
- An FFT was carried out over a window of 2^N samples, where $N = 5$ (32 data points = 320 m). The minimum suggested value of N is used, and by doing so we are exploring the smallest-scale roughness patterns possible (Brigham, 1988; Taylor et al., 2004; Bingham et al., 2007).
- Total bed roughness is then defined as the integral of the FFT of power spectra in each moving window. Li et al. (2010) defined this aspect of roughness as describing the vertical irregularity (ξ_t), and so it effectively reflects the amplitude of bed roughness. Wright et al. (2012) suggested that if the analysis is performed on the slope of the bed instead of its height, then this acts as a filter that reveals only short wavelength variations. The resulting slope roughness (ξ_{sl}), therefore, is a useful indicator of smaller-scale variations, which are otherwise masked by the large-scale bed roughness patterns that dominate standard methods of roughness assessment. The second parameter that Li et al. (2010) referred to is described as the frequency roughness parameter (η; cf., Wright et al., 2012), but here we refer to it as the roughness wavelength (η^{-1}). This is calculated as the total roughness divided by the roughness of the bed slope. Our approach to calculating these parameters was first tuned to a sample data set, as presented in Li et al. (2010), after which the same tuned approach was applied to our data.
- Roughness measurements were interpolated using the *topo to raster* procedure in ArcGIS (cf. Ross et al., 2014) onto a 1-km grid before being smoothed over a circular area with a radius of 10 km. In order to increase confidence in our interpolation, we do not display data that are >2500 m from a flightline.
- Finally, roughness values were normalised before being compared with measurements of ice velocity and overall bed topography in order to better understand the causes of observed roughness patterns.

2.3. Directionality of roughness

Another way of assessing roughness is to explore its directionality and relation to ice flow. This is useful because where bed roughness results from ice-dynamic processes, it is likely that roughness relative to the ice-flow field may vary considerably. Flow-related roughness anisotropy has been observed in several modern and former ice stream beds, as megascale glacial lineations (MSGLs) that can develop with their long axis parallel to ice flow (e.g., Graham et al., 2007). Numerous images of ice-sheet beds across deglaciated terrains (e.g., Clark, 1993; Stokes and Clark, 2001; Dowdeswell et al., 2006; Evans et al., 2006; Graham et al., 2007), and also an analysis of the ice-sheet bed mapped from radar transects across a contemporary ice-stream (King et al., 2009), show long strings of such streamlined landforms whose bed roughness transverse to flow might be expected to be considerably greater than that along flow. Consequently, a deep valley in which fast ice flow is carried where active movement of sediment, including erosion and deposition, dominates might be characterised by high orthogonal roughness but low parallel roughness, reflecting the presence of MSGL-like features (note, such features may also include bedrock surfaces featuring streamlined scouring/grooving (Bradwell et al., 2008)).

In order to explore directionality, we separate our survey lines into those that are approximately perpendicular and orthogonal to flow (Fig. 1B). Given that few of our lines are exactly parallel or orthogonal to flow direction, we allow for some fluctuation — up to ±25° of flow direction (or orthogonal to). The relative sparseness of the resulting datasets means that there are significant data gaps and so carrying out our FFT approach to determine roughness provides extremely patchy results with large gaps. As an alternative, we employ a simpler assessment of roughness, which uses the standard deviation (SD) of bed elevations as an indicator of roughness. This approach is more suitable for data sets without densely available data and has previously been applied before in a modified form (cf. Rippin et al., 2006). As an initial check on the validity of this approach, we mapped roughness derived using SD in comparison to roughness derived using FFT across the data domain. We found that the trends in roughness variation across the region are broadly consistent but that the magnitude of variation is dampened using the SD approach compared with the FFT one. This gives us confidence that the use of SD is an appropriate measure for the purpose of the roughness-directionality analysis, where the volume of input tracks is necessarily lower and degraded for FFT analysis by a proportionally greater number of breaks in the flightline tracks.

3. Results and analysis

The first analysis of bed roughness in the IIS area came from data collected in the 1970s, which had an along-track resolution of ~2 km, meaning that roughness could only be determined at a relatively coarse scale (cf., Jankowski and Drewry, 1981; Bingham and Siegert, 2007). To assess the relative coherence between our data and those collected previously, we first resampled our data at an equivalent 2000-m step size, and calculated total roughness (i.e. parameter 1) over an FFT window of 64 km length. The outcome of this comparison exercise is shown in Fig. 3.

Fig. 3 demonstrates that our new data reflects the same broad patterns that Bingham and Siegert (2007) identified and which led to this more detailed study. Namely, that the bed is remarkably smooth toward the grounding line and rougher inland where flow is slower. This preliminary result means that the total roughness measurement revealed by the two-parameter index is consistent with the original work of Bingham and Siegert (2007).

With the new data having much higher along-track resolution, we are able to assess roughness over windows of just 320 m length — 200 times higher resolution than with the 1970s' data. The ability to reveal roughness at this scale highlights some extraordinarily detailed patterns, as shown in Fig. 4, which we discuss below.

3.1. Total roughness

Much of the study region is dominated by relatively low roughness values (Fig. 4A). These are lowest to the north of the region (area marked as 'coastal basin' in Fig. 1A) and display generally higher roughness values to the south, particularly farther inland. In more detail, the Bungenstock Ice Rise (cf., Fig. 3B) and the main trunks of IIS and MIS (clearly visible to the left and right of the Bungenstock Ice Rise, respectively) are dominated by exceptionally low roughness values. There are three tributaries (A, B, and C) that feed into IIS, with tributary C also partly feeding into MIS. Here, the bed is deep and, notably, the beds of these tributaries are relatively smooth, but not as smooth as the faster flowing main trunk. Roughness along these feeder-tributaries is patchy with apparent variable total roughness along their lengths, reflecting the more variable bed topography found here and the existence of basins and troughs in these locations. Tributary B is less deep than A and C, but displays similar overall roughness characteristics. The upper reaches of the relatively smooth beds of tributaries A and B are

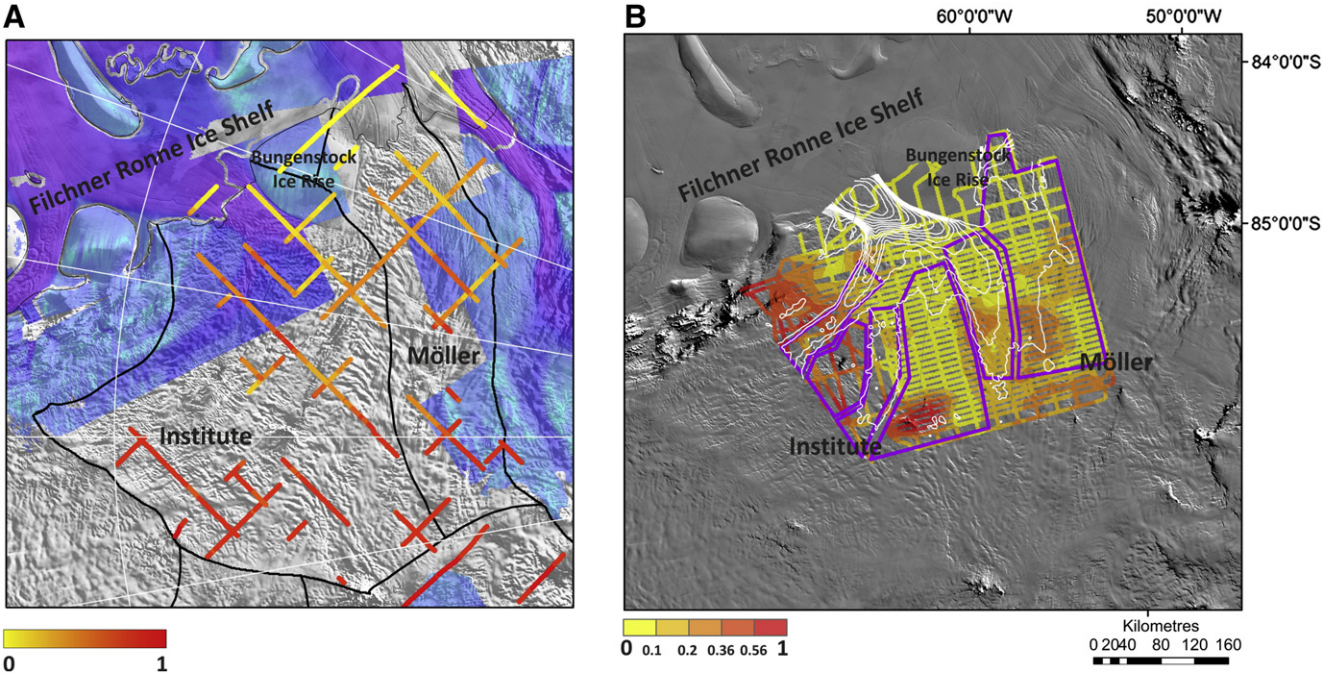

Fig. 3. Comparison of (A) original roughness map of IIS/MIS (adapted from Bingham and Siegert, 2007; their Fig. 1B) and (B) our new roughness estimates from high resolution data, degraded to an identical step size, and shaded using a similar colour scheme. Note that interpolation of roughness is limited to a 2.5-km buffer around flightlines. Purple boxes delineate our previously defined zones (see Fig. 1A for an indicator of the naming conventions for each area).

surrounded by significant subglacial mountain ranges (Pirrit Hills and Nash Hills) that are characterised by much higher roughness values (note the red areas located around these tributaries; cf., Fig. 1A). Such correspondence between subglacial mountains and higher roughness might be expected, as mountains are really just an end-member expression of roughness. Meanwhile, intertributary areas B–C and D are different — apart from a small region of very high roughness, terrain here is relatively high and also flat, experiences slow ice flow, and generally exhibits lower total roughness.

3.2. Wavelength roughness

For much of the IIS/MIS region, patterns of wavelength roughness closely replicate those of total roughness, such that where total roughness is higher, wavelength roughness is also higher, and conversely, where total roughness is lower, wavelength roughness is also lower (Fig. 4B). This relationship is most pronounced in the deep basin and intertributary area B–C (both low) and the Pirrit and Nash Hills (both high). However, one significant anomalous region exists where wavelength roughness is high but total roughness is low. This anomalous region (area A; Figs. 4A and B) actually has the highest wavelength roughness values — these are found in two distinct patches along the tributary.

3.3. Slope roughness

Slope roughness over much of the IIS/MIS region is low; in fact the extent of low slope roughness is greater than either total or wavelength roughness (Fig. 4C). Again, the largest areas of lower roughness are found in the deep coastal basin and in region B–C, as well as much of region D. Slope roughness is only high over the high ground identified as dominating area A–B, as well as high ground at the margins of tributaries A and B, particularly near the upper reaches of tributary A.

Table 1 summarises the roughness characteristics for the IIS/MIS region discussed above.

3.4. Roughness directionality

Figs. 5A and B show bed roughness determined parallel and orthogonal to ice flow, respectively. These images are less clear, but we observe that roughness parallel to flow (although somewhat patchy) is generally, and to varying degrees, lower within the faster flow tributaries and higher in intertributary areas. Conversely, within those same tributaries, roughness orthogonal to flow is, to varying degrees, somewhat higher. Two significant anomalies exist. Firstly, that area BC shows consistently low roughness in both directions. Secondly, an area of very low roughness (both directions) exists in the centre of Area A, which coincides closely with an area of local (albeit subdued) topography.

4. Discussion (characterisation of terrain)

Table 1 enables us to delineate clearly three different types of terrain as follows:

- Type I: regions that have **low** ξ_t but **high** η^{-1} and are characterised by deep trough-like subglacial topography and high velocities.
- Type II: regions that have **low** ξ_t and **low** η^{-1} and are characterised by either deep to moderately-deep trough-like subglacial topography and high ice velocities or by higher ground and lower ice velocities.
- Type III: regions that have **high** ξ_t and **low-to-moderate** η^{-1} and are characterised by significant subglacial mountains and low ice velocities.

In order to highlight the relationship between the two parameters of roughness, we plot [(normalised ξ_t) − (normalised η^{-1})] (hereafter referred to as ζ (zeta)) (Fig. 4D), which further highlights the classes identified above, with type I regions showing as green; type II regions as yellow/orange; and type III regions as orange/red. Li et al. (2010) provided a classification system with suggested geomorphic explanations for regions of bed that exhibit different high or low values for each of

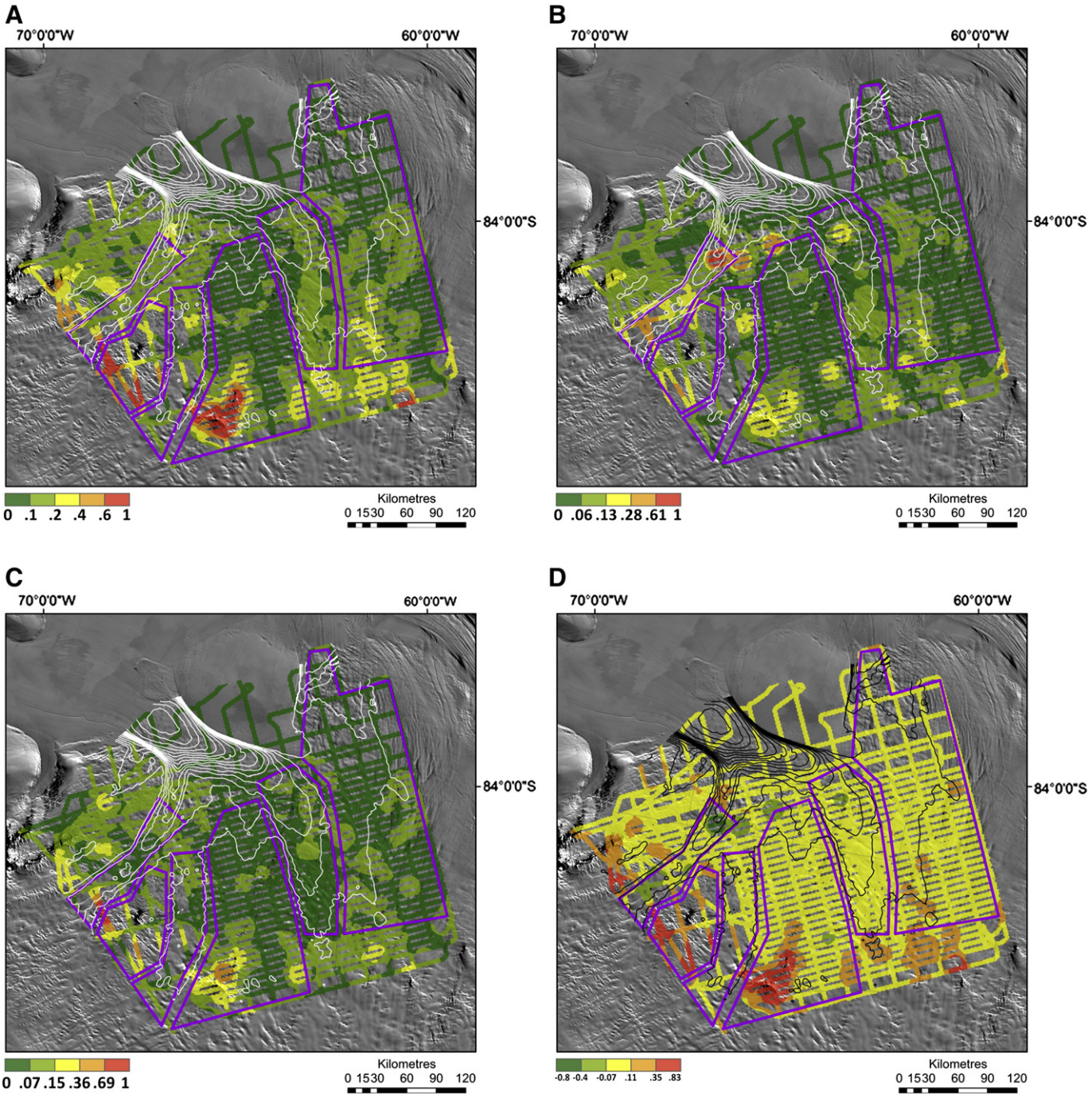

Fig. 4. Normalised (A) total (ξ_t); (B) wavelength (η^{-1}) and (C) slope (ξ_{sl}) roughness of the entire IIS/MIS region. In all three images, lower roughness areas are shaded green while higher roughness areas are shaded red. The background image is the MODIS mosaic of Antarctica (Haran et al., 2005; Scambos et al., 2007), and contours of InSAR velocities (after Rignot et al., 2011) are superimposed to indicate the location of the IIS and MIS. Purple boxes delineate our previously defined zones (see Fig. 1A for an indicator of the naming conventions for each area). (D) Plot of ζ which highlights regions of the bed with distinct roughness characteristics. Although we cannot interpret values of ζ precisely, clearly the lowest values (the dark green areas), which indicate where $\zeta \to -1$, represent type I regions. Similarly, the moderate values (the yellow areas), which indicate where $\zeta \to 0$, represent type II regions, while the highest values (the red and orange areas), which indicate where $\zeta \to +1$, represent type III regions.).

the two-parameter roughness values, which we are now able to critique.

4.1. Roughness explanation by region

In Table 1, we identified distinct regions based on the two-parameter characteristics. We now interpret these regions, incorporating also our findings about directionality of roughness.

4.1.1. Region type I

This region is characterised by low ξ_t and high η^{-1}, and incorporates just area A — this is the westernmost tributary feeding IIS (the Ellsworth trough). Low ξ_t implies lowered roughness peaks and high η^{-1} implies that long-wavelength roughness obstacles dominate. This is considered by Li et al. (2010) to be a product of the infilling of valleys with eroded sediments. Li et al. (2010) suggested that these characteristics are typical of a marine setting where intensive preglacial deposition of marine sediment has dominated (cf., Siegert et al., 2005). However, Wright

Table 1
Summary of parameters associated with the different regions indicated in Fig. 1A.

Area	Bed ele	Bed appearance	Ice vel	ξ_t	η^{-1}	ξ_{sl}	Type
A	Deep	Constrained valley	High	Mod low	High	Low	I
B	Mod deep	Shallow valley	High	Mod low	Mod	Mod low	II
C	Deep	Deep valley	High	Mod low	Mod low	Low	II
A–B	Shallow	High mountains	Low	High	Mod	High	III
B–C1[a]	Shallow	High mountains	Low	High	Mod	High	III
B–C2[a]	Shallow	High plateau	Low	Low	Low	Low	II
D1[a]	Deep	Low basin	Mod high	Low	Low	V.low	II
D2[a]	Shallow	Intersecting valleys	Low	Low	Low	Low	II
Deep basin	V. deep	Deep and wide area	High	V.low	V.low	V.low	II

[a] Note, areas B–C and D are each further subdivided into two distinct regions because of differing characteristics within them. Assessment of the two roughness parameters enables the designation of specific areas as a specific 'type' and these are discussed subsequently.

et al. (2012) contended that while intensive deposition that masks bedrock relief may be responsible for such characteristics, another possibility is that erosive processes have had an impact by reducing the amplitude of roughness obstacles. Our analysis and interpretation of roughness orientation in this region (i.e., lower parallel roughness but higher orthogonal roughness) lend further support for the suggestion that active basal processes are critically important. We envisage the presence of streamlined bedforms, similar to those identified by King et al. (2009) beneath the Rutford Ice Stream (west Antarctica). King et al. (2009) identified an alternating network of ridges and troughs, revealed only in the direction orthogonal to flow, and this work led to these features being identified as MSGLs, streamlined in the direction of ice flow, also displaying evidence of continuing modification and evolution. Such an interpretation would support the pattern of roughness orientation observed here. We suggest that some combination of sedimentation, sediment streamlining, and removal as well as perhaps some erosion and smoothing of bedrock has occurred in this area (Ross et al., 2012).

4.1.2. Region type II

Here, both roughness parameters are low in value — such characteristics are found in areas B, C, D, part of area B–C, and the deep coastal basin. Most of these areas are associated with fast flowing ice — tributaries of IIS (area B is the central tributary of IIS; area C is the easternmost tributary of IIS); a tributary of MIS (area D) and the trunk of IIS (the deep basin). However, this large-scale grouping masks some intriguing complexities as follows:

- Part of area BC has similar roughness properties to other region II areas, yet physically appears to be quite different — it is a high plateau with ice that is comparatively thinner than that found in the deep troughs.
- Area C has the most pronounced roughness orientation signature. Roughness here is highly anisotropic, suggesting the presence of streamlined bedforms.
- Ice velocities in area D are rather lower than in all the other areas. It is not dissimilar to area B–C in that it is a plateau surface but that it is also cut by a series of deep enclosed basins.
- The deep coastal basin is exceptionally smooth such that it is the area of lowest roughness (both parameters) and also exceptionally uniform with low roughness directionality values too.

Li et al. (2010) suggested that low ξ_t and η^{-1} are indicative of a landscape that has experienced intensive erosion but with minimal deposition. This is because where large wavelength features (large η^{-1})

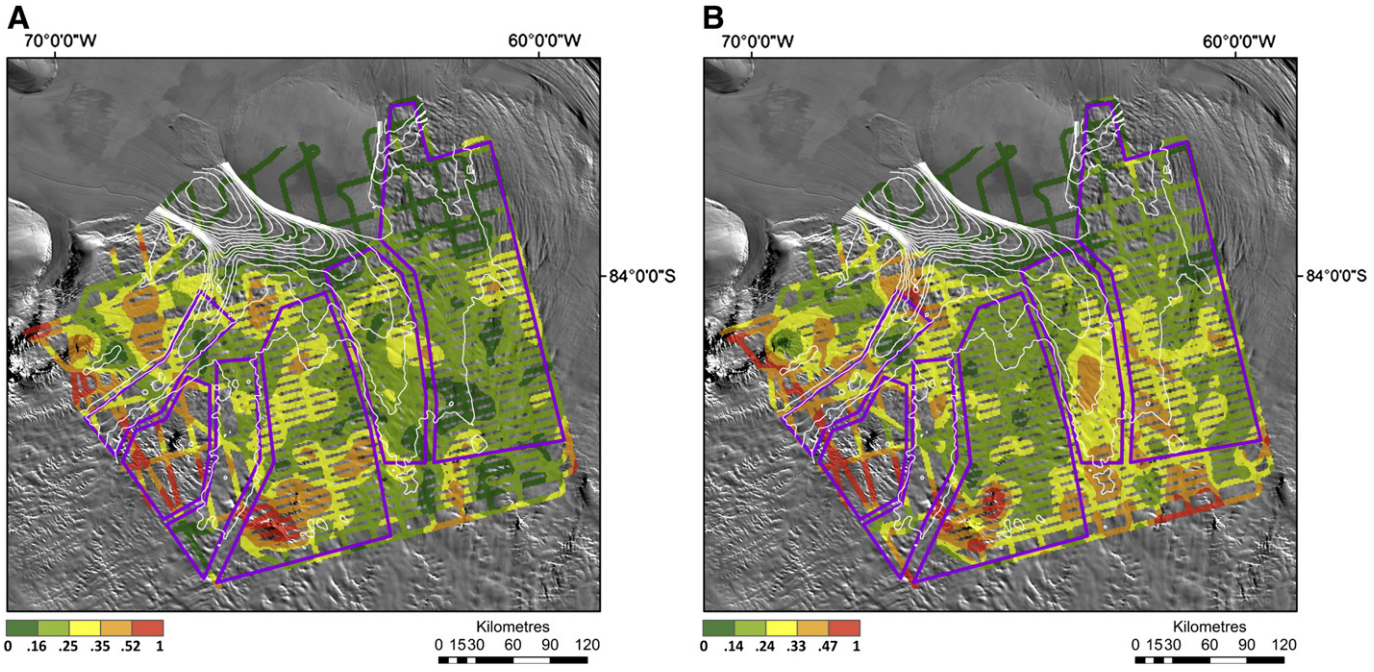

Fig. 5. Basal roughness determined using the standard deviation of along-track bed topography (A) parallel to flow and (B) orthogonal to flow. Roughness was calculated in both cases by identifying lines that were parallel or orthogonal to flow direction ±25° (cf., Fig. 1B). Standard deviations were then calculated over a rectangular moving window over the terrain of 300 × 300 m. These results were then interpolated onto a 1-km grid using the topo-to-raster routine in ArcGIS before being smoothed. Purple boxes delineate our previously defined zones (see Fig. 1A for an indicator of the naming conventions for each area).

dominate, this implies deposition and thus 'drowning' of smaller obstacles; but conversely, a small η^{-1} implies a lack of deposition as smaller wavelength features are still prominent. One might envisage a landscape cut by multiple shorter wavelength valleys with no infilling — and this is fitting for areas where ice flow is fast and warm (cf., Li et al., 2010). It is also an interpretation that is in keeping with the idea of streamlining of bed topography, as reflected in our roughness directionality experiment. Importantly though, such an interpretation does not explain the characteristics of area B–C or of the deep basin. In area B–C, roughness parallel to flow is relatively high (and less so orthogonally). A possible interpretation is that this region has not experienced significant streamlining of roughness obstacles. However, what roughness is apparent is nevertheless of shorter wavelengths and may arguably be a consequence of geomorphological processes that were active before ice sheet emplacement. This area might thus be protected from modification by slow-flowing ice under which erosion rates are small. Such an interpretation is consistent with the identification of preserved landforms associated with earlier periods of glaciation (e.g., Bo et al., 2009; Rose et al., 2013; Ross et al., 2014). By contrast, the deep coastal basin exhibits exceptionally smooth topography using all measures of roughness. Even though this region seems to indicate that short wavelength roughness obstacles dominate, we suggest that this signal is actually misleading because all other indicators suggest a very smooth topography that we interpret as being dominated by sediment emplacement. This basin was recently named the Robin Subglacial Basin; and radio-echo sounding data has suggested that it is underlain by thick marine sediments, most likely deposited during periods of warmer climate when ice cover was less extensive (Ross et al., 2012). This interpretation is also consistent with models of magnetic and gravity data, which suggest that a thick sedimentary basin is present in this region (Jordan et al., 2013).

4.1.3. Region type III

Here, both parameters are relatively high in value, a characteristic found in area A–B and parts of area B–C. These are intertributary regions that are slow-moving and are characterised by relatively thin ice and, in places, very rough subglacial terrain. Li et al. (2010) suggested that these roughness characteristics imply an area that has undergone neither significant erosion nor deposition. However, some deposition could have taken place; but the sediments emplaced are protected beneath cold-based, slow-moving ice that is nonerosive. We interpret these areas as being subglacial highlands (e.g., the Pirrit Hills) that were perhaps once eroded by the older, more restricted ice sheet suggested by Ross et al. (2014). We suggest that this rugged topography was then preserved by the thin (cold-based), slow-flowing ice conditions of the present ice sheet.

5. Conclusions and interpretation

We have presented an analysis of the roughness of subglacial topography from airborne RES data over the IIS/MIS region of west Antarctica, which has revealed important details and complexities in the processes that have acted, and are acting, beneath the ice in this region. Superficially, one might envisage the IIS/MIS area as one where a series of smooth-bedded ice-stream tributaries intersect rougher terrain where ice flow is much slower. Simpler roughness analysis techniques might indeed reveal this. However, our use of multiple techniques for exploring the roughness of IIS and MIS shows that this is a significant oversimplification and that, in fact, far more information can be extracted on the nature of the subglacial environment from analyses of basal roughness. Five different approaches to roughness calculations were used to comprehend former glacial conditions: (i) total roughness (ξ_t); (ii) roughness wavelength (η^{-1}); (iii) roughness slope (ξ_{sl}); (iv) roughness parallel to flow; and (v) roughness orthogonal to flow.

We have used roughness analysis to identify (i) tributaries and other locations where significant sediment deposition has occurred; (ii) tributaries underlain by topography that appear to exhibit streamlining; and (iii) locations that are currently protected from erosion, perhaps by cold basal ice, but bear the hallmarks of erosion under an older, more restricted ice sheet. Our work, therefore, helps to identify a subglacial landscape that has been modified to differing degrees and has also revealed the complexity of terrain beneath contemporary ice sheets. It also demonstrates that imprints of previous glacial activity can be preserved beneath ice masses, so that conditions at the bed reflect a combination of contemporary and historical processes. Finally, it also highlights the importance of factoring in the effects of streamlining of sediments and erosion when considering mechanisms responsible for forming a smooth bed. We suggest that future work should not depend solely on the pure application of the quantitative Li et al. (2010) approach of landscape analysis but should integrate it with informed and sensible geomorphic frameworks for landscape interpretation.

Acknowledgements

Funding was provided by the UK NERC AFI grant NE/G013071/1. Carl Robinson (Airborne Survey engineer), Ian Potten and Doug Cochrane (pilots), and Mark Oostlander (air mechanic) are thanked for their invaluable assistance in the field. We also thank two anonymous referees and the Editor, Richard Marston, for insightful comments that have helped to improve this paper.

References

Bingham, R.G., Siegert, M.J., 2007. Bed roughness characterization of Institute and Möller Ice Stream, west Antarctica: comparison with Siple Coast ice streams. Geophysical Research Letters 34, L21504. http://dx.doi.org/10.1029/2007GL031483.

Bingham, R.G., Siegert, M.J., 2009. Quantifying subglacial bed roughness in Antarctica: implications for ice-sheet dynamics and history. Quaternary Science Reviews 28, 223–236.

Bingham, R.G., Siegert, M.J., Young, D.A., Blankenship, D.D., 2007. Organized flow from the South Pole to the Filchner-Ronne ice shelf: an assessment of balance velocities in interior east Antarctica using radio echo sounding data. Journal of Geophysical Research 112, F03S26. http://dx.doi.org/10.1029/2006JF000556.

Bo, S., Siegert, M.J., Mudd, S.M., Sugden, D., Fujita, S., Xiangbin, C., Younyou, J., Xueyuan, T., Yuansheng, L., 2009. The Gamburtsev Mountains and the origin and early evolution of the Antarctic Ice Sheet. Nature 459, 690–693.

Bradwell, T., Stoker, M.S., Krabbendam, M., 2008. Megagrooves and streamlined bedrock in NW Scotland: the role of ice streams in landscape evolution. Geomorphology 97, 135–156.

Brigham, E.O., 1988. The Fast Fourier Transform and Its Applications. Prentice-Hall, Englewood Cliffs.

Catania, G., Hulbe, C., Conway, H., Scambos, T.A., Raymond, C.F., 2012. Variability in the mass flux of the Ross ice streams, west Antarctica, over the last millennium. Journal of Glaciology 58 (210), 741–752.

Clark, C.D., 1993. Mega-scale glacial lineations and cross-cutting iceflow landforms. Earth Surface Processes and Landforms 18, 1–29.

Corr, H., Ferraccioli, F., Frearson, N., Jordan, T., Robinson, C., Armadillo, E., Caneva, G., Bozzo, E., Tabacco, I., 2007. Airborne radio-echo sounding of the Wilkes subglacial basin, the Transantarctic Mountains, and the Dome C region. Terra Antarctica Reports 13, 55–64.

Dowdeswell, J.A., Evans, J., Ó Cofaigh, C., Anderson, J.B., 2006. Morphology and processes on the continental slope off Pine Island Bay, Amundsen Sea, West Antarctica. Geological Society of America Bulletin 118 (5), 606–619.

Drewry, D.J., 1983. Antarctica: Glaciological and Geophysical Folio. University of Cambridge, Scott Polar Research Institute, Cambridge.

Drewry, D.J., Meldrum, D.T., 1978. Antarctic airborne radio echo sounding, 1977–78. Polar Record 19 (120), 267–273.

Drewry, D.J., Meldrum, D.T., Jankowski, E., 1980. Radio echo and magnetic sounding of the Antarctic ice sheet, 1978–79. Polar Record 20 (124), 43–51.

Evans, J., Dowdeswell, J.A., Ó Cofaigh, C., Benham, T.J., Anderson, J.B., 2006. Extent and dynamics of the West Antarctic Ice Sheet on the outer continental shelf of Pine Island Bay during the last glaciation. Marine Geology 230, 53–72.

Fahnestock, M.A., Scambos, T.A., Bindschadler, R.A., Kvaran, G., 2000. A millennium of variable ice flow recorded by the Ross Ice Shelf, Antarctica. Journal of Glaciology 46, 652–664.

Graham, A.G.C., Lonergan, L., Stoker, M.S., 2007. Evidence for Late Pleistocene ice stream activity in the Witch Ground Basin, central North Sea, from 3D seismic reflection data. Quaternary Science Reviews 26, 627–643.

Haran, T., Bohlander, J., Scambos, T., Painter, T., Fahnestock, M., 2005. MODIS Mosaic of Antarctica (MOA) Image Map. Boulder, Colorado USA: National Snow and Ice Data Center. http://dx.doi.org/10.7265/N5ZK5DM5.

Hélière, F., Lin, C.-C., Corr, H., Vaughan, D., 2007. Radio echo sounding of Pine Island Glacier, west Antarctica: aperture synthesis processing and analysis of feasibility from space. IEEE Transactions on Geoscience and Remote Sensing 45 (8), 2573–2582.

Hubbard, B., Siegert, M.J., McCarroll, D., 2000. Spectral roughness of glaciated bedrock geomorphic surfaces: implications for glacier sliding. Journal of Geophysical Research 105 (B9), 21,295–21,303.

Hulbe, C., Fahnestock, M., 2007. Century-scale discharge stagnation and reactivation of the Ross ice streams, west Antarctica. Journal of Geophysical Research 112, F03S27. http://dx.doi.org/10.1029/2006JF000603.

Jankowski, E.J., Drewry, D.J., 1981. The structure of West Antarctica from geophysical studies. Nature 291, 17–21.

Jordan, T.A., Ferraccioli, F., Ross, N., Corr, H.F.J., Leat, P.T., Bingham, R.G., Rippin, D.M., Le Brocq, A., Siegert, M.J., 2013. Inland extent of the Weddell Sea Rift imaged by new aerogeophysical data. Tectonophysics 585, 137–160. http://dx.doi.org/10.1016/j.tecto.2012.09.010.

Kamb, B., 2001. Basal zone of the West Antarctic ice streams and its role in lubrication of their rapid motion. In: Alley, R.B., Bindschadler, R.A. (Eds.), The West Antarctic Ice Sheet: Behavior and Environment. Antarctic Research, Series, 77. AGU, Washington, D. C., pp. 157–199.

King, E.C., Hindmarsh, R.C.A., Stokes, C.R., 2009. Formation of mega-scale glacial lineations observed beneath a west Antarctic ice stream. Nature Geoscience 2 (8), 585–588.

Li, X., Sun, B., Siegert, M.J., Bingham, R.G., Tang, X., Zhang, D., Cui, X., Zhang, X., 2010. Characterization of subglacial landscapes by a two-parameter roughness index. Journal of Glaciology 56, 831–836.

Peters, M.E., Blankenship, D.D., Morse, D.L., 2005. Analysis techniques for coherent airborne radar sounding: application to west Antarctic ice streams. Journal of Geophysical Research 110, B06303. http://dx.doi.org/10.1029/2004JB003222.

Rignot, E., Mouginot, J., Scheuchl, B., 2011. Ice flow of the Antarctic Ice Sheet. Science. http://dx.doi.org/10.1126/science.1208336.

Rippin, D.M., 2013. Bed roughness beneath the Greenland ice sheet. Journal of Glaciology 59 (216), 724–732.

Rippin, D.M., Bamber, J.L., Siegert, M.J., Vaughan, D.G., Corr, H.F.J., 2006. Basal conditions beneath enhanced-flow tributaries of Slessor Glacier, east Antarctica. Journal of Glaciology 52 (179), 481–490. http://dx.doi.org/10.3189/172756506781828467.

Rippin, D.M., Vaughan, D.G., Corr, H.F.J., 2011. The basal roughness of Pine Island Glacier, west Antarctica. Journal of Glaciology 57 (201), 67–76.

Rose, K.C., Ferraccioli, F., Jamieson, S.S.R., Bell, R.E., Corr, H.F.J., Creyts, T., Braaten, D., Jordan, T.A., Fretwell, P.T., Damaske, D., 2013. Early east Antarctic Ice Sheet growth recorded in the landscape of the Gamburtsev Subglacial Mountains. Earth and Planetary Science Letters 375, 1–12.

Ross, N., Bingham, R.G., Corr, H.F.J., Ferraccioli, F., Jordan, T.A., Le Brocq, A., Rippin, D.M., Young, D., Blankenship, D., Siegert, M.J., 2012. Steep reverse bed slope at the grounding line of the Weddell Sea sector in West Antarctica. Nature Geoscience 5 (6), 393–396. http://dx.doi.org/10.1038/NGEO1468.

Ross, N., Jordan, T.A., Bingham, R.G., Corr, H.F.J., Ferraccioli, F., Le Brocq, A., Rippin, D.M., Wright, A.P., Siegert, M.J., 2014. The Ellsworth Subglacial Highlands: inception and retreat of the west Antarctic Ice Sheet. Geological Society of America Bulletin 126 (1–2), 3–15. http://dx.doi.org/10.1130/B30794.1.

Scambos, T., Bohlander, J., Raup, B., Haran, T., 2004. Glaciological characteristics of Institute Ice Stream using remote sensing. Antarctic Science 16, 205–213. http://dx.doi.org/10.1017/S0954102004001919.

Scambos, T., Haran, T., Fahnestock, M., Painter, T., Bohlander, J., 2007. MODIS-based Mosaic of Antarctica (MOA) data sets: continent-wide surface morphology and snow grain size. Remote Sensing of Environment 111 (2), 242–257. http://dx.doi.org/10.1016/j.rse.2006.12.020.

Siegert, M.J., Taylor, J., Payne, A.J., Hubbard, B., 2004. Macroscale bed roughness of the Siple Coast ice streams in West Antarctica. Earth Surface Processes and Landforms 29 (13), 1591–1596.

Siegert, M.J., Taylor, J., Payne, A.J., 2005. Spectral roughness of subglacial topography and implications for former ice-sheet dynamics in East Antarctica. Global and Planetary Change 45 (1–3), 249–263.

Stokes, C.R., Clark, C.D., 2001. Palaeo-ice streams. Quaternary Science Reviews 20, 1437–1457.

Taylor, J., Siegert, M.J., Payne, A.J., Hubbard, B., 2004. Regional scale roughness beneath ice masses: measurement and analysis. Computers and Geosciences 30 (8), 899–908.

Thiel, E., 1961. Antarctica, one continent or two? Polar Record 10 (67), 335–348.

Tulaczyk, S., Kamb, B., Scherer, R.P., Engelhardt, H.F., 1998. Sedimentary processes at the base of a west Antarctic ice stream: constraints from textural and compositional properties of subglacial debris. Journal of Sedimentary Research 68 (3), 487–496.

Vaughan, D.G., Corr, H.F.J., Ferraccioli, F., Frearson, N., O'Hare, A., Mach, D., Holt, J.W., Blankenship, D.D., Morse, D.L., Young, D.A., 2006. New boundary conditions for the West Antarctic ice sheet: subglacial topography beneath Pine Island Glacier. Geophysical Research Letters 33 (9), L09501. http://dx.doi.org/10.1029/2005GL025588.

Wright, A.P., Young, D.A., Roberts, J.L., Schroeder, D.M., Bamber, J.L., Dowdeswell, J.A., Young, N.W., Le Brocq, A.M., Warner, R.C., Payne, A.J., Blankenship, D.D., van Ommen, T.D., Siegert, M.J., 2012. Journal of Geophysical Research 117, F01033. http://dx.doi.org/10.1029/2011JF002066.